

MICRO FRICTION STIR WELDING OF COPPER ELECTRICAL CONTACTS

Received – Primljeno: 2014-01-24

Accepted – Prihvačeno: 2014-05-20

Original Scientific Paper – Izvorni znanstveni rad

The paper presents an analysis of micro friction stir welding (μ FSW) of electrolytic tough pitch copper (CuETP) in a lap and butt joint. Experimental plan was done in order to investigate the influence of tool design and welding parameters on the formation of defect free joints. The experiments were done using universal milling machine where the tool rotation speed varied between 600 and 1 900 rpm, welding speed between 14 and 93 mm/min and tilt angle between 3° and 5°. From the welds samples for analysis of microstructure and samples for tensile tests were prepared. The grain size in the nugget zone was greatly reduced compared to the base metal and the joint tensile strength exceeded the strength of the base metal.

Key words: micro friction stir welding (μ FSW), Cu ETP, tensile test, microstructure

INTRODUCTION

Components for electrical and electronic devices are usually made of oxygen-free copper (Cu OF), electrolytic tough pitch copper (Cu ETP), oxygen-free electronic copper (Cu OFE) or oxygen free phosphorus copper (Cu OFP) due to their high electrical conductivity, high thermal conductivity and the ability to work harden. Since these components are usually connected to other components their joining is needed. These coppers could be joined using different joining technologies [1]. Bolting and riveting is used when dismantling is needed. Adhesive bonding is applied when low joint strength is needed and smaller electrical and thermal conductivity is acceptable. Soft or hard brazing is selected based on the joint type and joint strength needed [1]. Fusion welding (manual metal arc welding, tungsten inert gas welding, metal inert gas welding, plasma gas welding, electron beam welding, laser welding) is used when high joint strength and high electrical conductivity is needed [2]. Electrical resistance welding enables moderate lap joint strength but is difficult due to high electrical conductivity of the joint [3, 4]. Ultrasonic welding, vibrational welding, friction welding (linear, rotational, friction stir welding (FSW)) enables good joint properties (electrical and thermal conductivity, strength) and are usually used for high production series in tight tolerances. Diffusion welding is slow but enables good joint properties [5]. Roll bonding is applicable for high production series while cold pressure welding is usually used for extension of different pro-

files [1, 6, 7]. The process can be used for joining other materials like Al-alloys where a good knowledge of material data is of highest importance for forming process [8] and further use of the component [9]. For roll bonding process quality tool steels [10, 11] are used due to their exposure to high working temperatures.

At fusion welding fusion defects can occur due to high thermal conductivity of copper, therefore preheating is necessary for thicknesses above 3 mm, when using argon shielding. In the heat-affected zone (HAZ) of wrought Cu ETP high temperatures could permit diffusion and migration of oxide particles causing the porosity in HAZ. A rapid welding is thus needed to restrict overall heating. At shielding gas welding deoxidation is prevented using argon, helium or nitrogen shielding gasses.

The selection of optimal technology depends on many factors especially on the size of the production series, joint types and joint properties needed.

FSW of copper requires much higher heat input compared to welding of aluminium alloys due to greater dissipation of heat through the workpiece [12-14]. At lower heat input weld defects like elongated cavities usually occur but at higher heat input oxidation of weld surface is present [13]. FSW has been successfully used to weld 50 mm thick copper canisters for containment of nuclear waste [15].

FSW welding of Cu ETP at temperatures between 460 – 530 °C enables formation of sound welds, with ~ 70 HV and strains three times longer than in the base metal [16, 17]. Defect free FSW welds were also obtained with low heat input FSW at which the joint ultimate tensile strength achieved almost 100 % of the base metal [18]. The fracture mechanisms and characteristics for four regions were also defined. Leal et al. [19] established that the torque, the microstructure, hardness and

D. Klobčar, J. Tušek, Faculty of Mechanical Engineering, University of Ljubljana, Ljubljana, Slovenia; M. Bizjak, Faculty of Natural Sciences, University of Ljubljana, Ljubljana, Slovenia; V. Lešer, Faculty of Health Sciences Novo mesto, Na Loko 2, Novo mesto, Slovenia

the formation of weld defects are influenced mainly by tool rotation speed and in less by the traverse speed and shoulder cavity. Analysis of friction stir processing (FSP) of Cu-DHP showed that the tool geometry, processing parameters and heat exchange conditions determine grain size and mechanical properties of stirred zone. The grain size increases with decreasing traverse speed, and with increasing rotational speed [20].

The paper presents an analysis of μ FSW of Cu ETP in a lap and butt joint. In the study we explored the influence of tool design and welding parameters. The results showed that the grain size in the nugget zone is greatly reduced compared to the base metal and the joint tensile strength was thus improved.

EXPERIMENTAL WORK

A standard Cu ETP with temper R290 with its nominal chemical composition $\geq 99,9\%$ Cu and $0,005 - 0,04\%$ O was used [21]. Its yield strength was ≥ 250 MPa and tensile strength 290 - 360 MPa. The test coupons were 2 mm thick with dimensions 110×25 mm. They were welded in a lap joint (LJ) and butt joint (BJ) (Figure 1). A universal milling machine was used for μ FSW and welding was done in position control. Welding tools were made from 1.2343 (X38CrMoV5-1) tool steel quenched and tempered to 45 HRC. The concave shoulders of the tool B and C were 6 mm in diameter and of the tool A and D 4 mm in diameter. Tool A had conical shaped pin with 2,5 mm in diameter and 1,8 mm long. Tool B and C had a pyramid shaped pin with 3 mm square 3 mm and 1,8 mm long. Tool D had square block pin 1,2 mm square and 1,5 mm long. The tool rotated clockwise and moved in the centre of the test coupons. Experimental plan was done where tool rotation speed (ω) varied between 600 and 1 900 rpm, welding speed (v) varied between 14 and 93 mm/min and tilt angle between 3° and 5° .

Weld surface appearance was visually examined. From the welds samples for microstructure analysis and tensile test were sectioned. The prepared samples for macro and microstructure analysis were etched in a solution of FeCl_3 and examined using a light optic microscope with the digital camera for picture acquiring.

The heat input was determined using rotation per feed ($\text{RPF} = \omega/v$), which presents simplified pseudo heat index.

RESULTS AND DISCUSSION

Figure 1 shows macrosections of FSW copper coupons welded in a butt joint using tool A. The welding was done at 37 mm/mm travel speed, with 3° tool tilt and with different RPF heat inputs. Visual examination of the weld surface appearance showed no traces of poor welds (Figure 1a). The macrosections revealed that elongated cavities formed at the advancing side (AS) of the tool and that cavity cross section is decreasing with

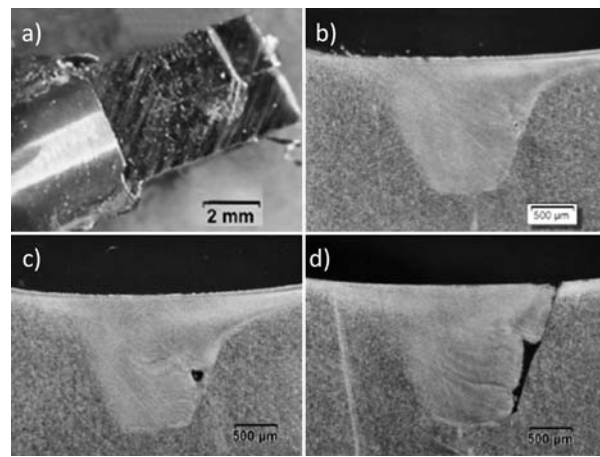


Figure 1 The influence heat input during FSW (at 37 mm/min welding rate, using tool A) on appearance of elongated cavities; a) FSW welded sample, b) RPF = 51,3 rev/mm, c) RPF = 31,9 rev/mm and d) RPF = 16,2 rev/mm

higher RPF. The cavity appeared at the AS due to bigger travel speed difference (different workpiece/tool traveling direction) even though the temperatures are higher at AS. These defects were formed due to too small heat input at small 4 mm tool shoulder diameter at which the majority of frictional heat is generated.

For the next series of experiments the pin shape was changed from conical to pyramid and block in order to increase heat generation due to deformation of the material around the tool pin.

Figure 2 shows the weld surface appearance after FSW with different tools, parameters and joint configurations. Welds on Figure 2a and 2c were done with similar tool design (different pin length), the same welding parameters, and lap and butt joint configuration. The weld surface oxidized at the lap joint (Figure 2a) since higher temperature was generated due to smaller heat

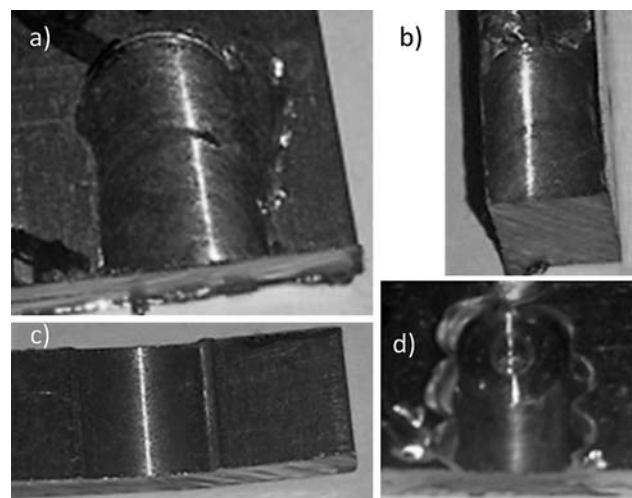


Figure 2 FSW weld surface appearance: a) lap joint (tool B, RPF = 20,4 rev/mm, 93 mm/min, 3°), b) butt joint (tool D, RPF = 135,7 rev/mm, 14 mm/min, 5°), c) butt joint (tool C, RPF = 20,4 rev/mm, 93 mm/min, 3°) and d) butt joint (tool D, RPF = 135,7 rev/mm, 14 mm/min, 5°)

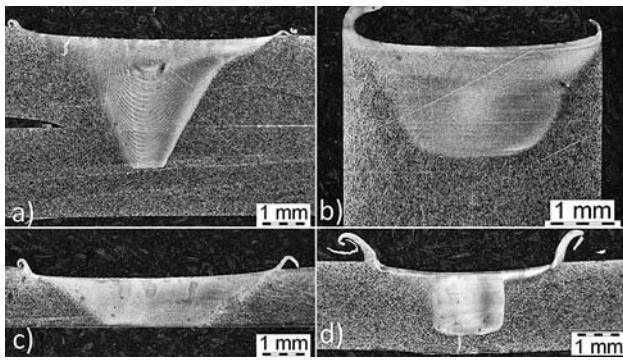


Figure 3 FSW weld macrostructure of a) lap joint (tool B, RPF = 20,4 rev/mm, 93 mm/min, 3°), b) butt joint (tool D, RPF = 135,7 rev/mm, 14 mm/min, 5°), c) butt joint (tool C, RPF = 20,4 rev/mm, 93 mm/min, 3°) and d) butt joint (tool D, RPF = 135,7 rev/mm, 14 mm/min, 5°)

conduction to the bottom coupon, while weld surface at butt joint did not oxidized, due to quicker heat dissipation through side coupons. Butt welds on Figure 2b and d were done with the same welding tool and parameters and with the test coupons positioned in a lap and butt configuration. The welding was done with smaller heat input and weld surface oxidation in lap position was less pronounced while in butt position was not present. The reason for this difference is in heat dissipation from under the shoulder to the test coupons.

Figure 3 shows the macrosections of the welds from the Figure 2. The produced welds had no welding defects. The “onion rings” showing rotations of material under the tool shoulder are visible at Figure 3a.

Figure 4 shows microsection of the lap weld welded with tool A. An elongated cavity and fitting of the coupons is shown at Figure 4a. From the Figure 4b and c it could be noted that the grain size in the stir zone is greatly reduced, similarly as reported by others authors [20].

The tensile tests were done on butt welds. The joint strengths obtained were between 272,3 MPa (Figure 3c) and 419,3 MPa (Figure 3d). The weld achieved higher strength than the base material (290 – 360 MPa) due to improved weld microstructure by thermo-mechanical FSP.

CONCLUSIONS

The following conclusions can be summarized:

- Heat input and joint type affect on the heat dissipation and the weld surface oxidation.
- Pyramid and block shaped tool pins generates more heat with deformation of the material around the pin and have an advantage over conical or cylindrical pins.
- In the stir zone the grain size is reduced due to thermo-mechanical FSP which could improve mechanical strength of the weld.
- Welding defects like elongated cavities are formed at the advancing side due to the different workpiece/tool traveling direction at smaller heat inputs.

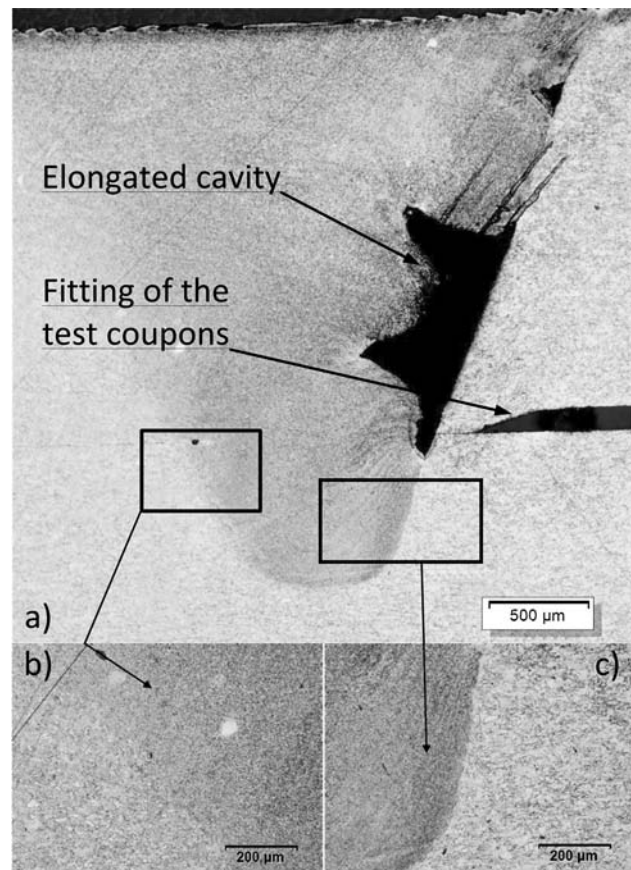


Figure 4 FSW weld microstructure (tool A, RPF = 10,1 rev/mm, 116 mm/min, 3°): a) the whole weld, and the interface between stirred zone and base metal b) retreating side and c) advancing side of the tool

Acknowledgments

The authors wish to thank Nataša Rant, Nika Breskvar, Boris Bell and Tomaž Martinčič for the help at experimental work. The research was sponsored by Slovenian Research Agency under the grant L2-4183.

REFERENCES

- [1] L. Brown, CDA Publication No 98, (1994), 1-64.
- [2] M. Pleterski, J. Tušek, T. Muhič, L. Kosec, *J. of Mater. Sci. & Technol.*, 27 (2011) 8, 707-713.
- [3] J. S. Agapiou, T. A. Perry, *J. of Manuf. Proc.*, 15 (2013) 4, 549-557.
- [4] S. Simončič, P. Podržaj, *Meas. Sci. Technol.*, 23 (2012) 6, 1-7.
- [5] A. A. Shirzadi, E. R. Wallach, *Sci. Technol. Weld. Join.*, 9 (2004) 1, 37-40.
- [6] M. Gojič, L. Vrsalović, S. Kožuh, A. C. Kneissl, I. Anžel, S. Gudić, B. Kosec, M. Klišković, *J. Alloys Comp.*, 509 (2011) 41, 9782-9790.
- [7] H. Dyja, S. Mróz, A. Milenin, *J. Mater. Proc. Technol.*, 153-154 (2004), 100-107.
- [8] T. Pepelnjak, V. Magoč, B. Barišič, *Metalurgija*, 51 (2012) 2, 153-156.
- [9] M. Šimic, M. Debevec, N. Herakovič, *J. Mech. Eng.*, (in print), DOI:10.5545/sv-jme.2013.1104.
- [10] J. Brnič, M. Čanađija, G. Turkalj, D. Lanc, T. Pepelnjak, B. Barišič, G. Vukelić, M. Brčić, *Mater. Manuf. Process.* 24 (2009) 7/8, 758-762.

- [11] A. Nagode, G. Klančnik, H. Schwarczova, B. Kosec, M. Gojić, L. Kosec, *Eng Fail. Anal.*, 23 (2012), 82-89.
- [12] R. Nandan, T. DebRoy, H.K.D.H. Bhadeshia, *Progress Mater. Sci.*, (2008) 980-1023.
- [13] J. Teimournezhad, A. Masoumi, *Sci. Technol. Weld. Join.*, 15 (2010) 2, 166-170.
- [14] W. M. Thomas, K. I. Johnson, C. S. Wiesner, *Adv. Eng. Mater.*, 5 (2003) 7, 485-490.
- [15] L. Cederqvist, C. D. Sorensen, A. P. Reynolds, T. Öberg, *Sci. Technol. Weld. Join.*, 14 (2009) 2, 178-184.
- [16] Y. M. Hwang, P. L. Fan, C. H. Lin, *J. Mater. Proc. Technol.*, 210 (2010) 12, 1667-1672.
- [17] W.-B. Lee, S.-B. Jung, *Mater. Letters*, 58 (2004) 6, 1041-1046.
- [18] H. J. Liu, J. J. Shen, Y. X. Huang, L. Y. Kuang, C. Liu, C. Li, *Sci. Technol. Weld. Join.*, 14 (2009) 6, 577-583.
- [19] R. M. Leal, N. Sakharova, P. Vilaça, D. M. Rodrigues, A. Loureiro, *Sci. Technol. Weld. Join.*, 16 (2011) 2, 146-152.
- [20] I. Galvao, A. Loureiro, D. M. Rodrigues, *Advanc. Mater. Resear.*, 445 (2012), 631-636.
- [21] Wieland-K32, in, *Wieland*, pp. 2.

Note: The responsible translator for English language is Urška Letonja Grgeta, Moar. Prevajanje, Podgora, Slovenia